Organic Aerosol Mixing Observed By Single Particle Mass Spectrometry.

ARTICLE *in* THE JOURNAL OF PHYSICAL CHEMISTRY A · OCTOBER 2013

Impact Factor: 2.69 · DOI: 10.1021/jp405789t · Source: PubMed

3 AUTHORS, INCLUDING:

Ellis Shipley Robinson
University of Colorado Boulder
8 PUBLICATIONS **87** CITATIONS
SEE PROFILE

Neil M Donahue
Carnegie Mellon University
270 PUBLICATIONS **10,562** CITATIONS
SEE PROFILE

THE JOURNAL OF PHYSICAL CHEMISTRY A

Feature Article

pubs.acs.org/JPCA

Organic Aerosol Mixing Observed by Single-Particle Mass Spectrometry

Ellis Shipley Robinson, Rawad Saleh, and Neil M. Donahue*

Center for Atmospheric Particle Studies, Carnegie Mellon University, 5000 Forbes Avenue, Pittsburgh, Pennsylvania 15213, United States

Supporting Information

ABSTRACT: We present direct measurements of mixing between separately prepared organic aerosol populations in a smog chamber using single-particle mass spectra from the high-resolution time-of-flight aerosol mass spectrometer (HR-ToF-AMS). Docosane and docosane-d_{46} (22 carbon linear solid alkane) did not show any signs of mixing, but squalane and squalane-d_{62} (30 carbon branched liquid alkane) mixed on the time scale expected from a condensational-mixing model. Docosane and docosane-d_{46} were driven to mix when the chamber temperature was elevated above the melting point for docosane. Docosane vapors were shown to mix into squalane-d_{62}, but not the other way around. These results are consistent with low diffusivity in the solid phase of docosane particles. We performed mixing experiments on secondary organic aerosol (SOA) surrogate systems finding that SOA derived from toluene-d_8 (a surrogate for anthropogenic SOA (aSOA)) does not mix into squalane (a surrogate for hydrophobic primary organic aerosol (POA)) but does mix into SOA derived from α-pinene (biogenic SOA (bSOA) surrogate). For the aSOA/POA, the volatility of either aerosol does not limit gas-phase diffusion, indicating that the two particle populations do not mix simply because they are immiscible. In the aSOA/bSOA system, the presence of toluene-d_8-derived SOA molecules in the α-pinene-derived SOA provides evidence that the diffusion coefficient in α-pinene-derived SOA is high enough for mixing on the time scale of 1 min. The observations from all of these mixing experiments are generally invisible to bulk aerosol composition measurements but are made possible with single-particle composition data.

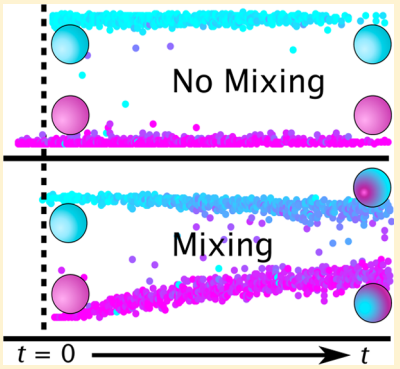

INTRODUCTION

We care about fine particles (aerosol) in the atmosphere for three main reasons: they kill people, they have strong but uncertain climate effects, and they can make it very hard to see. Fine particles are central to three of the top 10 leading causes of mortality in the global burden of disease,[1] and roughly 50 000 people per year die in the US from inhalation of excessive levels of fine particles in ambient air.[2] The aerosol indirect effect couples particles to climate via cloud droplet numbers. The associated changes to cloud droplet number, and thus cloud albedo, from preindustrial times are one of the largest climate forcing uncertainties.[3] Additionally, direct scattering of light also has a significant climate effect.[3] Finally, haze is simply difficult to see through. When the horizon is obscured, it poses a threat to pilots; this may have been the cause of the small plane crash that claimed the lives of John F. Kennedy Jr. and his companions in 1999.[4]

Aerosol is a suspension of particles and vapor, and tropospheric aerosol is a complex mix of inorganic and organic components whose physical and chemical characteristics depend strongly on source, location, and atmospheric age, among many other factors.[5] The organic fraction, which comprises a large percentage of aerosol mass, between 20 and 90%,[6] is poorly understood relative to the inorganic fraction. Organic species in atmospheric aerosol cover a wide range of molecular weights, polarities, and volatilities.[7] Due to the large number and variety of molecules in tropospheric organic aerosol (OA), thermodynamic predictions of individual equilibrium vapor pressures and miscibilities in this complex mixture are for practical purposes impossible.

The partitioning of organic constituents plays a crucial role in determining the chemical composition and physical characteristics of particles, as well as the evolving gas-phase chemistry, an important mechanism for chemical aging in OA.[8] Whether there exists a single organic phase or multiple organic phases should have dramatic consequences for the partial pressures of any organic molecules in the system, as species in a mixture have greatly reduced equilibrium vapor pressures compared to their pure reference phase, via Raoult's Law. Thus it is extremely important in predictions of aerosol mass and composition to know how many organic phases are present in aerosol systems found in the atmosphere.

Most regional-scale modeling studies assume an internally mixed aerosol. This assumption means that all particles of the same size have the same composition. Furthermore, if models treat semivolatile organics, most assume that those organics

Received: June 11, 2013
Revised: October 7, 2013
Published: October 16, 2013

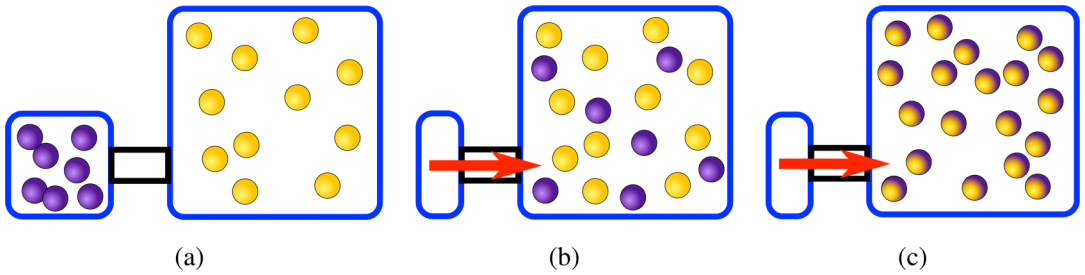

Figure 1. Schematic for mixing experiments. (a) Aerosol populations are prepared in separate chambers prior to the mixing event. (b) Extreme cases of mixing behavior, where the two populations exist as completely separate phases (no mixing). (c) The two populations mixed via gas-phase exchange (complete mixing).

form a single phase, which is typically treated as distinct from a second inorganic (sometimes called aqueous) phase. That organic condensed phase is assumed to be in equilibrium with the gas phase. Implicit in this assumption is that diffusion into the condensed organic phase is fast compared to gas-phase diffusion. Recent experimental studies call into question whether this can be true,[9−11] and thus whether an internally mixed aerosol can be assumed for atmospheric models. The process of mass exchange between two organic aerosol populations can shed light on the diffusion time scales within aerosol particles. If mixing is observed on a rapid time scale, then, unambiguously, diffusion limitations are not present in the system. Conversely, when mixing does not occur, it may point to mass-transfer barriers, including, but not limited to, low condensed-phase diffusivity.

In this work, we describe experimental techniques for performing aerosol mixing experiments and demonstrate the use of single-particle mass spectrometry for determining whether two aerosol populations mix. This technique is applied first to mixing experiments between single-component aerosol populations that cleanly demonstrate both the vapor pressure-driven mixing process, as well as observations of phase separation in OA systems. The technique is then applied to atmospherically relevant mixing situations, to determine the mixing behavior between biogenic secondary organic aerosol (SOA) with both anthropogenic SOA and primary organic aerosol (POA).

BACKGROUND

There have been numerous studies experimentally addressing the question of whether mixed-OA systems have single or multiple phases. A wide range of conclusions has been drawn from those studies about general particle behavior in the atmosphere based either on explicit modeling of the results or on inferences invoked to explain discrepancies between expectations and observations. Song et al.[12] used yield data from SOA formation on organic seed particles to infer whether there was a single organic phase, or a core−shell phase-separated morphology in their smog chamber experiments. They concluded that SOA derived from α-pinene oxidation did not mix with dioctyl phthalate (DOP). Hildebrandt et al.[13] used a similar experimental design to conclude that SOA from α-pinene oxidation and SOA from toluene oxidation mix to form a single phase. Vaden et al.,[14] using the more direct method of single-particle mass spectrometry, observed phase separation in an α-pinene SOA/DOP system. Asa-Awuku et al.[15] found that initially phase-separated SOA from α-pinene oxidation and diesel exhaust OA collapsed into a single organic phase in a smog chamber experiment, inferred from size-distribution measurements of tracer fragments in the high-resolution time-of-flight aerosol mass spectrometer (HR-ToF-AMS). Using a thermodenuder, Cappa and Wilson[16] identified lubricating oil particles coated with α-pinene SOA as a two-phase system, having "side-by-side" morphologies.

Most of the OA mixing studies described above relied on inference to identify the number of organic phases present, with the exception of Vaden et al.'s single-particle measurements. Observing submicrometer phase separation directly is analytically very challenging, but the measurements are of utmost importance. Measuring OA mixing is highly related to another research question as well, regarding the condensed-phase diffusivity of molecules in OA particles. Recent research has questioned whether the dynamics of OA mixing would allow it to take place on atmospheric time scales, even when the constituents favor a single phase at equilibrium.[10,11,17] If OA exists as a glassy solid, with a high internal viscosity and low internal molecular diffusivity, the time scale for mixing might be long relative to the average atmospheric lifetime of an OA particle. Thus, any observations of OA mixing are potentially related to the phase state of OA particles as well.

Two processes can move material between organic particles: coagulation and condensation (gas-phase diffusion). Coagulational mixing is straightforward: as shown in Figure 1b, the collision between two different particles (yellow and purple) will result in one "new" particle with a mixed composition. This new particle will of necessity be larger than either of the two original particles. However, at the number concentrations of the experiments we shall describe here (as well as much of the atmosphere), coagulation is not a significant mixing process. If the aerosol is semivolatile, then condensational mixing must be considered as well. When semivolatile organics are associated initially with two different particle populations that are later brought together, if those compounds favor a single condensed phase at equilibrium, they will tend to mix within every particle across both (initially dissimilar) populations.[18] This "Marcolli mixing" occurs through gas-phase diffusion and could rapidly blur the distinction between particles emitted from various organic-rich sources (wood burning, vehicles, cooking, etc.) while at the same time redistributing secondary organics among the particle population.

Mixing can mean many things for particles. Particle populations can be said to be "well mixed" if particles have similar compositions, and particles of the same size are "internally mixed" if their compositions are all identical. However, well-mixed particle populations can still contain particles with complex morphologies and multiple distinct phases in each particle. A common example is the existence of distinct "organic" and "aqueous" phases (liquid−liquid phase

separation) for particles containing organic compounds that are not above some critical oxidation threshold.[19−21]

Here we are interested in the mixing of different organic constituents within and among particles. Many organic compounds associated with aerosols are thought to be semivolatile, meaning significant fractions are found in both the condensed and vapor phases at equilibrium.[22−24] This applies to both SOA[25] and POA.[26] SOA is often initially formed via gas-phase oxidation and subsequent condensation of oxidation products to particles;[27] thus whether or not different secondary compounds form a single phase at equilibrium, they will tend to wind up on all particles present when they are being formed.

EXPERIMENTAL DESIGN

Overview of Environmental Chamber Mixing Experiments. We conducted a series of mixing experiments, all following a common design depicted in Figure 1. Experimental details are listed in Table 1. For each mixing experiment, two aerosol populations were prepared separately, each in a chamber isolated from the other. As shown in Figure 1a, one aerosol population was formed in a 100 L Teflon sample bag, and the other was formed in a 10 m^3 Teflon chamber. This is similar to the procedure used by Asa-Awuku et al.,[15] and different from other SOA mixing studies where there is some sort of sequential aerosol preparation in the same volume.[12,13] This accomplished the following goals: first, in the case of SOA, the SOA precursor was given enough time to completely react with its oxidation source prior to the event of mixing. Second, all aerosols, both pure-component and SOA, were given time to reach thermodynamic equilibrium so that they were no longer growing by condensation. Only after each population was determined to be in equilibrium were the contents of the smaller chamber transmitted (via compression) into the larger chamber. Further changes in the system after this transfer can thus be attributed to mixing.

Table 1. List of Mixing Experiments

exp	10 m^3 smog chamber	100 L sample bag	mixing?
1	docosane	docosane-d_{46}	N
2	docosane-d_{46}	docosane	Y (w/ heating)
3	SOA (toluene-d_8 + OH, as seed)	squalane	N
4	squalane-d_{62}	squalane	Y
5	–	SOA (α-pinene + O_3)	–
6	SOA (toluene-d_8 + OH, as seed)	SOA (α-pinene + O_3)	Y

In all experiments presented here, one of the aerosol sources (either the pure-component aerosol or the SOA precursor) was prepared from a fully deuterated compound. This ensures separability in the mass spectra between the two organic aerosols in each mixing experiment and provides unique tracer ions that can be used to determine the source of any particle.[13]

Aerosol Preparation. Aerosol preparation and characterization procedures used in this study are similar to those used in previous smog-chamber experiments conducted at Carnegie Mellon University (CMU).[13,28] Prior to each experiment, all chambers were flushed continuously for >12 h with clean, dry air (cleaned with HEPA, silica-gel, and activated-carbon filters in series) to ensure low background particle, organic vapor, and water concentrations. All experiments were performed at low (<5%) relative humidity and room temperature (298 K). Background particle concentrations were less than 10 particles cm^{-3} for each experiment.

SOA was formed by either the ozonolysis of α-pinene or the photo-oxidation of deuterium-substituted toluene (toluene-d_8) with added OH. α-Pinene SOA was formed in the 100 L chamber by injecting a liquid aliquot of the precursor into a heated tube fit with an airtight septum. Clean, dry air carried the vaporized α-pinene into the 100 L chamber, which was previously charged with excess ozone. No seed particles were used in the α-pinene SOA experiments because the nucleated particles reached a sufficient size (vacuum aerodynamic diameter (D_{va}) > 180 nm) to be seen with the light scattering laser in the AMS. For toluene-d_8 SOA formation, nitrous acid (HONO) was used as an OH source for photo-oxidation. Toluene-d_8 was added to the 10 m^3 chamber using a septum injector and swept into the chamber with clean, dry air. HONO was added to the chamber by bubbling filtered air through a nitrous acid solution for 15 min. Ultraviolet lights were turned on to initiate toluene-d_8 photo-oxidation but were turned off prior to the mixing event. Ammonium sulfate seeds were used for all toluene-d_8 SOA experiments to provide surface area for condensable organic vapors. Initial ammonium sulfate concentrations for experiments with seed particles were 2000 cm^{-3} and had a count median diameter of approximately 100 nm. This ensured that toluene-d_8 SOA particles would be large enough for detection by the light scattering module. Seed particles were generated through atomization of 1 g/L $(NH_4)_2SO_4$ solution, followed by a silica-gel diffusion dryer and a 2 mC neutralizer before the particles entered the chamber.

Pure-component organic particles were prepared by flash vaporization. A small, resistive metal heater enclosed in a stainless steel sheath was used to flash the organic material into the chamber, where aerosol particles were formed by homogeneous nucleation. To perform this flash vaporization, an aliquot of the organic material was placed on the stainless steel surface before the heater was inserted into the chamber on the end of a long tube. With a flow of clean, dry dispersion air used to mix the chamber, the heater was power-cycled until the organic material completely evaporated. The resulting vapor plume cooled rapidly via mixing in the chamber, developing a sufficient supersaturation to drive nucleation and rapid growth of pure particles.

Ensemble particle volume and number concentrations were measured with a scanning mobility particle sizer (SMPS, TSI classifier model 3080, CPC model 3772 or 3010). Ensemble particle composition and mass were measured with a high-resolution time-of-flight aerosol mass spectrometer (HR-ToF-AMS; Aerodyne Research, Inc.) operated in the single-reflection V-mode. Single-particle mass spectra were taken with an HR-ToF-AMS operated in light scattering single-particle (LSSP) mode, which has been described in detail before.[29,31] We discuss briefly the use of the LS mode for this application below.

Operation of HR-ToF-AMS in Single-Particle Mode. Single-particle mass spectra for particles with D_{va} greater than 180 nm were acquired by operating the HR-ToF-AMS in LSSP mode. For all experiments, the HR-ToF-AMS was operated according to the following procedure: The HR-ToF-AMS alternated between V-mode, which provides ensemble average mass spectra (MS) and size-resolved composition data (PToF,

dx.doi.org/10.1021/jp405789t | J. Phys. Chem. A 2013, 117, 13935−13945

particle time-of-flight), and LSSP mode, which provides single-particle sizing and composition information, for 60s each.

The construction and operation of the light scattering module for the ToF-AMS has been fully described elsewhere.[29,31] Briefly, the instrument consists of a continuous wave laser (405 nm, 50-mW; CrystaLaser, LC BCL-050-405) that crosses the collimated particle beam at a right angle within the time-of-flight region of the instrument. During LSSP and PToF operation, a chopper at just after the aerosol lens constitutes the beginning of the PToF region. During the large majority of chopper cycles, either zero or one particle traverses the PToF region. In the LSSP mode, scattered light from sampled particles is collected by an ellipsoidal mirror with one focus at the particle−laser intersection point and the other at the photocathode of a photomultiplier tube. The scattering signal provides two important pieces of information: first, pulse timing measures the flight time between the chopper and the laser providing the particle vacuum aerodynamic diameter. Second, the pulse also triggers the collection of individual mass spectra over the entire chopper cycle. This is necessary because data cannot be acquired and processed continuously and triggering on light scattering reduces the data rate to a manageable load.

Data from the LSSP mode were processed using custom software.[30] The software classifies particles based on how they interact with the vaporizer, sorting particles into "prompt", "delayed", and "null" events. Prompt particles are operationally defined as those particles whose signal arrives within 20% of the predicted time on the basis of the velocity calculated from the chopper-to-laser distance and the measured light scattering pulse. Delayed particles are all particles whose MS signals deviate by more than 20% of the predicted arrival time, and null particles are those with a scattered light signal but no detectable MS signal.[31]

We used the following parameters for data processing: a scattering threshold (signal-to-noise) of five to reject events with low scattered light intensity,[31] and an operationally defined MS threshold of 15 collected ions for each particle to be considered for MS analysis. Before sorting particles into "prompt", "delayed", and "null" events. Our results were not sensitive to our MS threshold, though it should be noted that this value is between the two MS thresholds used in Liu et al.[31] (6 ions for collection efficiency calulations and 40 ions for clustering). Particle coincidence (i.e., multiple particles entering the ToF region of the instrument per chopper cycle) at the number concentrations of these experiments was minimal but can be identified from the scattered light signal. All coincident particles were filtered by the software, and not considered in the analysis.

Our analysis and separation of single-particle mass spectra relies on using the cosine similarity between two vectors (each of which represent a mass spectrum):

$$\cos(\theta) = \frac{\vec{A}\cdot\vec{B}}{\|\vec{A}\|\|\vec{B}\|} \quad (1)$$

This correlation coefficient ranges from zero to one, where values close to one represent vectors with a small angle between them, or a high degree of similarity. Values close to zero represent vectors with a high angle of separation and low similarity. For the mass spectra of single particles, this quantity reflects whether particles in an ensemble are chemically similar to a chosen reference spectrum (or not). We have selected chemicals for our mixing experiments that exploit the use of cosine similarity. Because there exists a high degree of separability between isotopically labeled and nonlabeled aerosol mass spectra,[13] cosine similarity is able to completely segregate into clusters the different particles in these mixing experiments.

RESULTS AND DISCUSSION

Observations of External Mixtures. The mixing behavior between populations of docosane aerosol (prepared in the 10 m^3 smog chamber) and docosane-d_{46} aerosol (prepared in the 100 L sample bag) is shown in Figure 2. The top panel of

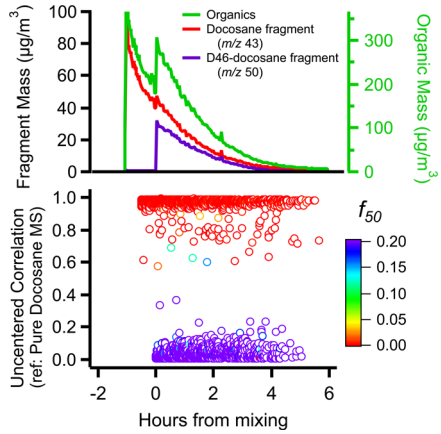

Figure 2. Time evolution of the mixing state between aerosol populations of docosane and docosane-d_{46}. The top panel shows the time series of marker mass spectral fragments m/z 43 (docosane) and m/z 50 (docosane-d_{46}), and the total organic mass from the time of the mixing event from the HR-ToF-AMS running in V-mode. The bottom panel shows uncentered correlation coefficients for all prompt single-particle mass spectra. The reference mass spectrum is docosane-d_{46}. The plot shows two chemically distinct populations that do not mix after 5 h of being in the same chamber.

Figure 2 shows the time series for two tracer mass spectral fragments unique to each type of particle: m/z 50 ($C_3D_7^+$) for docosane-d_{46} and m/z 43 fragment ($C_3H_7^+$) for docosane. All measurements were from the 10 m^3 smog chamber (the "mixing chamber"). Roughly 1 h before mixing the two populations, docosane particles were formed in the mixing chamber via flash vaporization, shown by appearance of m/z 43 in the top panel of Figure 2. Docosane-d_{46} particles were then introduced into the mixing chamber from the smaller bag, shown by the appearance of m/z 50. The particles were then left undisturbed in the mixing chamber for five hours.

The bottom panel of Figure 2 shows the correlation coefficient of each prompt single-particle MS compared to the reference spectrum of docosane-d_{46}, plotted as a function of time, calculated using eq 1. Particles are colored by the fraction of a tracer ion to the total ion number according to the following equation:

$$f_{m/z_i} = \frac{\text{no. of ions at } m/z_i}{\text{total no. of ions}} \quad (2)$$

(e.g., f_{43} = no. of ions at m/z 43/total no. of ions). Only particles with 150 ions or more are shown on this plot for clarity, though this filter does not affect our result. Prior to mixing, the particles all have very low correlation coefficients. At t = 0, a new population of particles is visible, with very high correlation to the docosane-d_{46} reference. Two very distinct

dx.doi.org/10.1021/jp405789t | J. Phys. Chem. A 2013, 117, 13935−13945

populations remain present in the chamber until the end of the experiment. All mixing experiments follow this same experimental and presentation scheme.

There were no changes in the correlation coefficients of the two populations, meaning that no significant mixing occurred. Similarly, when we manually separate the two groupings and look at their average mass spectra at the end of the experiment (Figure 3), there are no changes with time; no marker fragments from either aerosol are seen in the other grouping's mass spectrum.

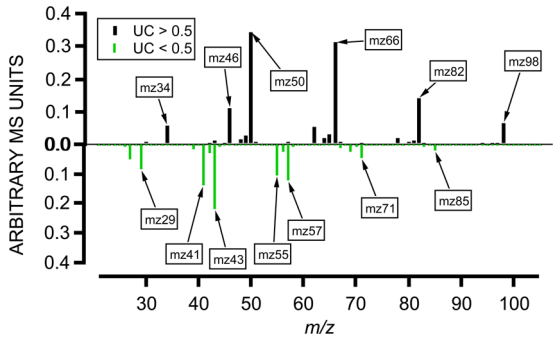

Figure 3. Average mass spectra for each particle population at t = 4 h that shows particles with uncentered correlation (UC) coefficient >0.5 are initially pure docosane-d_{46} and particles with UC < 0.5 are initially pure docosane. The mass spectrum of each population has almost no fragments in common with the other.

We ran simulations to ascertain whether coagulation was significant in all of our experiments as a mixing process. Using a sectional coagulation model, we compared the amount of particles coagulating into a given size bin with the total number of particles in that bin. Figure S1, Supporting Information, shows this comparison for the docosane/docosane-d_{46} experiment. The number of particles coagulating into the bin is so small compared to the total number of particles in the bin that coagulation can be ignored as a significant mixing process. This is confirmed by the complete lack of any significant evolution in the mass spectra for the two populations during this experiment. This is true for the rest of the experiments presented as well, which have similar number concentrations. That docosane and docosane-d_{46} do not show mixing is perhaps surprising. The docosane/docosane-d_{46} system should have near ideal-solution behavior, as the two constituents are functionally identical. Mixing is thus driven purely by entropy. We have simulated this experiment using a coupled aerosol- and gas-phase model, which is presented in Figure S2, Supporting Information. The time scale for condensational mixing for docosane, assuming no barriers to mass transfer, should be on the order of minutes. The saturation concentration of solid docosane at T = 293.15 K is estimated to be C^{sat} = 25 μg m^{-3} for the conditions of these experiments.[32]

We hypothesize that the mixing barrier in this case is either low molecular diffusivity in the condensed phase or low mass accommodation, due to the solid phase of docosane (and docosane-d_{46}) at the temperature of this experiment. Accommodation coefficients, α, of several orders of magnitude below unity have been reported for crystalline solids.[33] In fact, $\alpha \leq 10^{-4}$ is required to explain the observation here. To test this hypothesis, the experiment was repeated with an additional step where the smog chamber temperature was increased from 25 to 46 °C 2 h after the mixing event. The melting point of docosane is 44 °C. Figure 4 shows a sharp transition from two

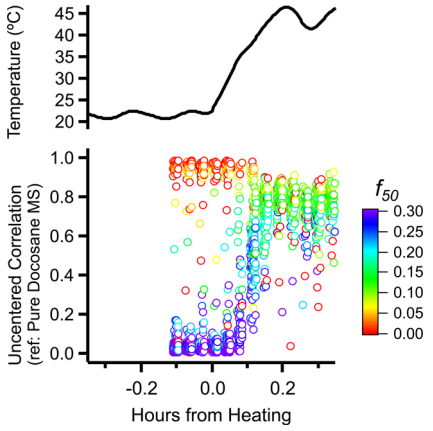

Figure 4. Time evolution of mixing between docosane and docosane-d_{46} with smog chamber heating. The white gaps are the sampling periods where the HR-ToF-AMS is operating in ensemble V-mode. With the increase of temperature, the two distinct populations rapidly mix into a single phase.

separate particle populations to a single population of mixed composition when the smog chamber reaches its maximum temperature. Although the entropic driving force is high for vapors of one compound to condense into particles of the other in both of these experiments, the solid phase makes the particles unavailable to accept vapors on the time scale of the experiment. The same barrier is not present when the particles are liquid, and in this case we do see mixing. These data emphasize the value of single-particle composition data, as this result would otherwise have been invisible to bulk composition measurements.

We also validated this hypothesis with a mixing experiment between squalane and docosane-d_{46} (presented in Figure S3, Supporting Information). Docosane-d_{46} particles were prepared initially in the larger smog chamber, and squalane particles were moved from the 100 L bag into the smog chamber to initiate mixing. Docosane-d_{46} vapors were taken up rapidly at 25 °C by squalane particles, which presented no diffusion limitation to absorption, due to their liquid-phase state. Squalane vapors were not observed to move into the docosane particles even though our condensational-mixing model showing that they should if the accommodation coefficient were high (Figure S4, Supporting Information). This further supports our conclusion that docosane is volatile enough to mix through the gas phase under typical ambient conditions, but that mass transfer or diffusion limitations prevent docosane particles from absorbing molecules from the gas phase.

We also observe a persistent external mixture in a similar mixing experiment between SOA formed via oxidation of toluene-d_8[13] and pure squalane particles, the results of which are shown in Figure 5. Both of these aerosol types are often used as atmospheric surrogates in smog chamber studies. SOA formed from toluene oxidation SOA is commonly used as a laboratory surrogate for anthropogenic SOA,[34] whereas squalane is extremely low vapor pressure oil and is used to represent hydrophobic POA.[12] Because the liquid squalane particles will take up vapors rapidly if thermodynamics favors it (as with docosane), this suggests that the limitation comes from the toluene-derived SOA. Either the SOA simply has very low

dx.doi.org/10.1021/jp405789t | J. Phys. Chem. A 2013, 117, 13935−13945

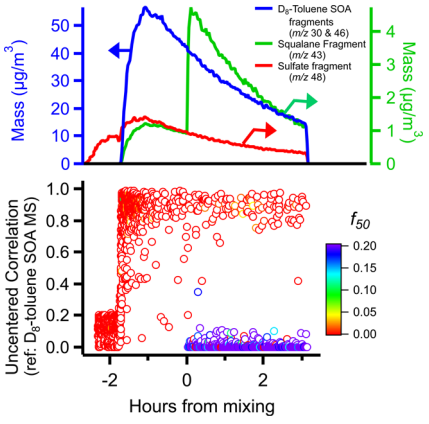

Figure 5. Time evolution of mixing state between aerosol populations of squalane and toluene-d_8 secondary organic aerosol with single-particle data colored by f_{43}. The reference mass spectrum is toluene-d_8 SOA. The two particle populations remain distinct over the course of the experiment.

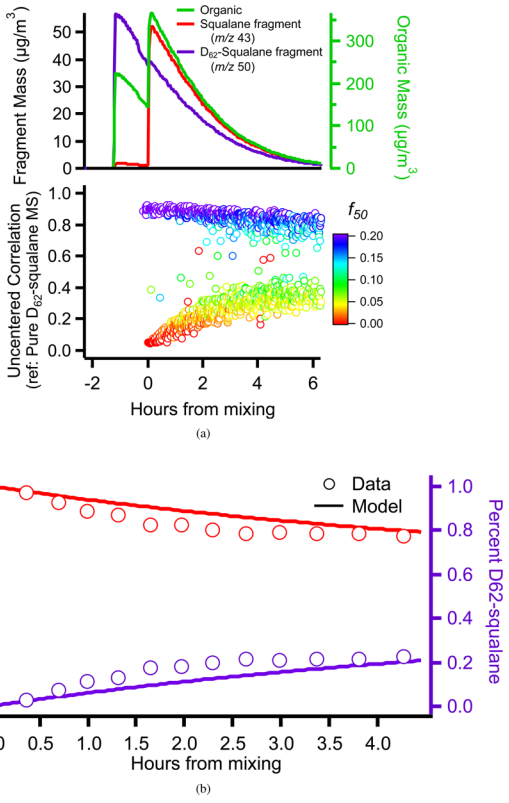

Figure 6. Time evolution of the mixing state between aerosol populations of squalane and squalane-d_{62}. (a) Squalane-d_{62} reference mass spectrum. (b) Time series of mass percent of squalane and squalane-d_{62} for the particle population that was initially pure squalane.

volatility and thus no vapors to add to the squalane particles, or mixing is simply not favored.

The correlation coefficients (reference toluene-d_8 SOA) for the two populations remain completely segregated hours after they are combined, meaning there is no significant mixing between the two condensed phases (bottom panel of Figure 5). Note also that the correlation coefficients of the ammonium sulfate seed particles are low compared to the SOA formed from toluene-d_8 oxidation reference spectrum. These low-coefficient particles begin to disappear as soon as the toluene-d_8 oxidation is initiated, providing single-particle evidence of organic oxidation products coating the salt seed particle. We also calculated coagulation to be insignificant for this experimental time scale.

Unlike the docosane/docosane-d_{46} experiment, this result is completely expected. Squalane, a long-chain branched alkane, is very likely immiscible with the oxidation products comprising the SOA from toluene-d_8, functionalized molecules such as epoxides and diols.[35] These results are consistent with those reported by Song et al.,[12] who saw no yield enhancement for biogenic SOA (α-pinene + O_3) in the presence of surrogate POA seed (dioctyl phthalate), evidence they used to conclude that SOA and POA form separate phases. Our result indicates that anthropogenic SOA and hydrophobic POA do not mix, though whether this should be extrapolated from the laboratory to the atmosphere is unclear. Regardless, these data demonstrate that smog chamber mixing experiments with single-particle data can be used to answer such questions of atmospheric significance.

Observations of Vapor Pressure-Driven Mixing. We performed an identical mixing experiment with populations of squalane and squalane-d_{62} particles, the results of which are shown in Figure 6a. Unlike the docosane mixing experiment, we see clear evidence of mixing between squalane and squalane-d_{62}, even though the vapor-pressure driving force for squalane ($C^{sat} = 8 \times 10^{-2}$ $\mu g\ m^{-3}$ at $T = 293.15$ K[32]) is much lower than even the solid phase of docosane. There is clear evolution in the chemical composition of the two visible particle populations over the course of the experiment, as shown in Figure 6a. Only particles with 150 ions or more are shown on this plot for clarity, though this filter does not affect our result.

We manually separated the two particle groupings into different categories (one with a correlation coefficient less than 0.5, the other greater than 0.5). The average mass spectra for each grouping is calculated for the first 30 min after the aerosol populations are mixed together and at $t = 4$ h, shown in Figure 7. These average single-particle mass spectra closely resemble the pure mass spectra of squalane-d_{62} and squalane collected with standard V-mode operation of the HR-ToF-AMS in calibration experiments (Figure S5, Supporting Information). At $t = 4$ h, the prominent peaks in each grouping at $t = 0$ have grown into the mass spectrum of the opposite grouping (for instance, m/z 50 ($C_3D_7^+$) is initially absent in the squalane grouping but is significant at $t = 4$ h). With this manual method, we are thus able to quantify the extent to which the two populations have mixed as a function of time. Using a simple chemical mass balance approach, we calculate the mass percent of the two chemicals in each aerosol population:

$$\text{percent A} = \frac{f_{m/z_i}}{f_{m/zi_{\text{pure},t=0}}} \quad (3)$$

By the end of the experiment (4.5 h from the mixing event), the initially pure-squalane particles are 78% percent squalane and 22% squalane-d_{62} by mass whereas the "squalane-d_{62} particles" are 58% percent squalane and 42% percent squalane-d_{62}. This time evolution of the mass percent of each compound in the initially-pure particles is presented in Figure 6b. The same condensational-mixing model is applied to this squalane mixing experiment, which is also plotted in Figure 6b. The agreement

dx.doi.org/10.1021/jp405789t | J. Phys. Chem. A 2013, 117, 13935−13945

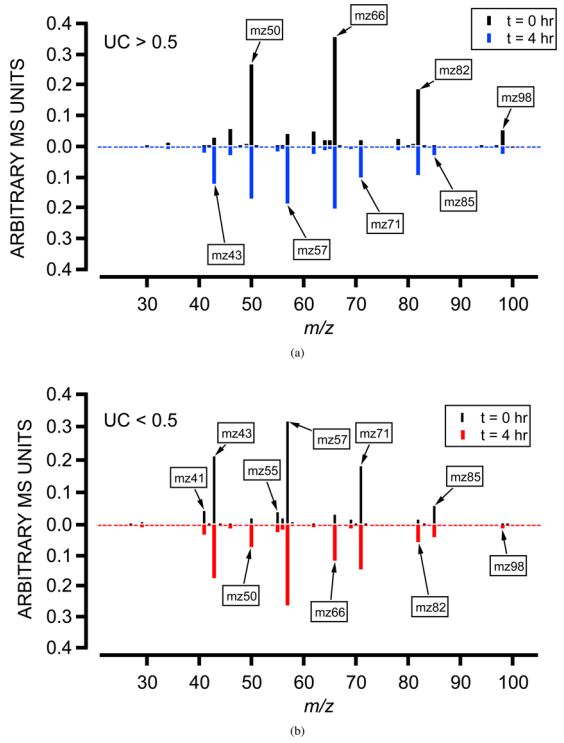

Figure 7. Average mass spectra for each particle population at $t = 0$ and $t = 4$ h. (a) Particles with UC > 0.5 (initially pure squalane-d_{62}). (b) Particles with UC < 0.5 (initially pure squalane). The MS at $t = 4$ h for each (a) and (b) show tracer fragments unique to the other pure component showing up in the average mass spectrum.

between the model and the data indicate that squalane exhibits ideal mixing, with no accommodation limitations, as expected.

Though the mixing is "expected" on the basis of our modeling, it is worth noting how counterintuitive this is. Squalane is a 30 carbon molecule with a saturation concentration of roughly 10^{-2} μg m^{-3} and yet within a few hours these molecules will wander from particle to particle under ambient conditions. This serves to emphasize just how sticky a molecule must be to remain more or less firmly on or in ambient particles; it must be much less volatile than glucose or paraffin wax.[8] This is also why the vast majority of primary aerosol emissions from combustion sources such as internal combustion engines, open burning, and cooking are in fact quite volatile.[36] The gas phase, in turn, is a dangerous place for large hydrocarbons and they are oxidized rapidly.[37] Compounds used as molecular markers of specific sources, such as levoglucosan used to identify wood burning, decay rapidly due to gas-phase attack by hydroxyl radicals.[38] This oxidation in turn often produces lower volatility products that are sticky enough to remain (at least partly) in the condensed phase and thus form secondary (oxidized) organic aerosol.[23,39]

The squalane experiment is a clear demonstration of both the process and time scale of condensational mixing. However, it is also a situation where single-particle composition data are the only type of data that can reveal this process, as the size-distributions for squalane and squalane-d_{62} are completely coincident. Asa-Awuku et al.[15] use noncoincident mass distributions (from PToF-mode) to reveal that diesel-exhaust POA can dissolve into α-pinene SOA. Their analysis, however, relies on the distributions being initially distinct, so that movement of material from one mode to another can be seen. In the above experiment, due to the coincidence of the size distributions, this mixing behavior is thus invisible, and no conclusions about mixing can be made. In such situations, only single-particle mass spectra can elucidate mixing behavior using data from an AMS.

Correlation plots can also be used to visualize mixing dynamics in these chamber studies. Figure 8 shows the

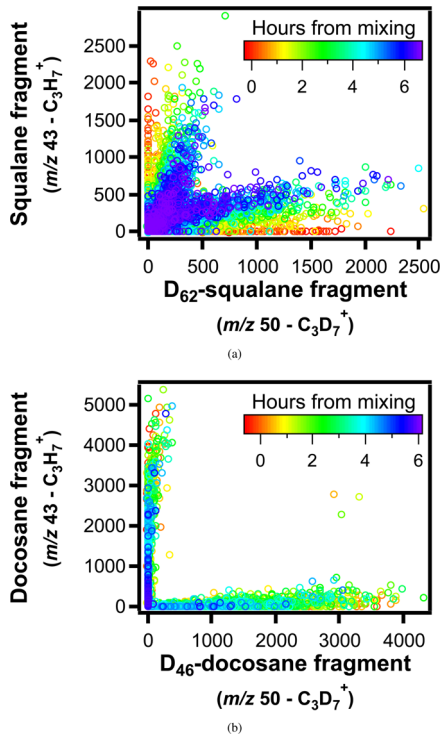

Figure 8. Correlation plots between marker mass spectral fragments (arbitrary units) with the color-scale indicating the time in the experiment (red = beginning, purple = end). (a) Docosane (m/z 43 marker) and docosane-d_{46} (m/z 50 marker) mixing experiment. (b) Squalane and squalane-d_{62} mixing experiment. Note particles are gaining signal from the opposite marker with time.

correlation of mass spectral tracer fragments for each aerosol population colored by time from the mixing event. In the docosane case (Figure 8a), there is a high degree of anticorrelation between each tracer, which persists for the entire experiment. On the other hand, for squalane we see the two distinct vectors converging over time as each aerosol population picks up molecules of the other from the shared vapor phase.

Observation of Mixing Between α-Pinene-Derived SOA and Toluene-Derived SOA. Having established our ability to observe mixing (or the absence of mixing) in several systems, we now turn to the mixing behavior of SOA derived from two important precursors associated with anthropogenic and biogenic emissions: toluene and α-pinene, respectively. SOA from α-pinene was prepared by ozonolysis in a 100 L sample bag. SOA from isotopically labeled toluene was formed in a 10 m^3 smog chamber by OH oxidation, similar to the previously described experiment. α-Pinene SOA was then added to the larger smog chamber. Single-particle mass spectra were correlated with a reference mass spectrum for SOA derived from toluene-d_8 to assess mixing behavior. The system, including the isotopic labels, is identical to the one described in Hildebrandt et al.,[13] except those authors formed the two SOA

dx.doi.org/10.1021/jp405789t | J. Phys. Chem. A 2013, 117, 13935−13945

in a single chamber, with one type serving as a condensation seed for the other. Here we formed the two populations separately and followed their mixing after chemistry reached its completion.

As a control, shown in Figure 9a, we first injected SOA derived from α-pinene oxidation into a clean smog chamber.

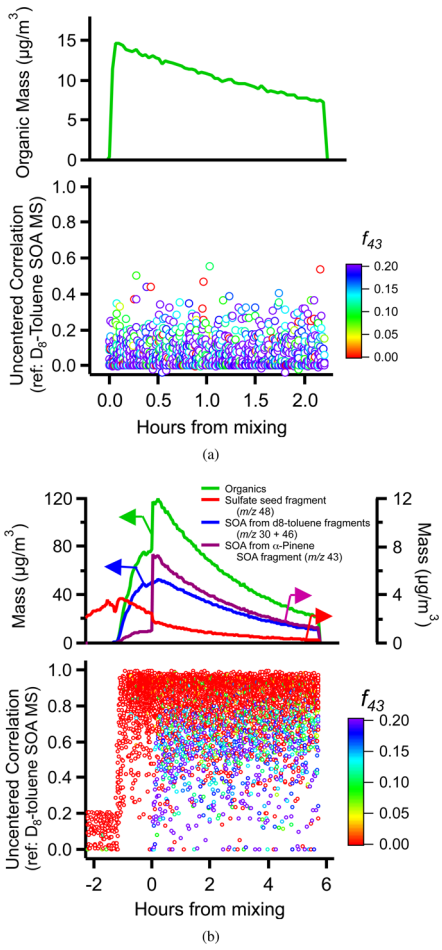

Figure 9. (a)Time series of α-pinene SOA control dilution experiment. The reference mass spectrum is toluene-d_8 SOA. (b) Time series of mixing experiment between α-pinene SOA and toluene-d_8 SOA. The reference mass spectrum is toluene-d_8 SOA. Note that the particles containing high amounts of m/z 43 are much more closely correlated with the toluene-d_8 reference than with α-pinene SOA diluted into a clean chamber).

The lower panel plots the correlation coefficient of these particles with reference to SOA derived from toluene-d_8, which remains near zero throughout the 2 h experiment. However, as shown in Figure 9b, when the same α-pinene-derived SOA particles were injected into a smog chamber containing SOA derived from toluene, the mass spectra of those α-pinene particles rapidly developed a strong correlation with the reference spectrum. This indicates that a significant mass of condensable vapors from the toluene-d_8 mixed into the particles derived from α-pinene.

The histogram in Figure 10a shows the distribution of f_{43} for these two experiments. There is a clear reduction in the fraction of m/z 43, as toluene-d_8 oxidation products have condensed onto these particles and now contribute new fragments to the single-particle MS. There is no contribution of m/z 43 to the SOA derived from toluene oxidation, shown by the green trace

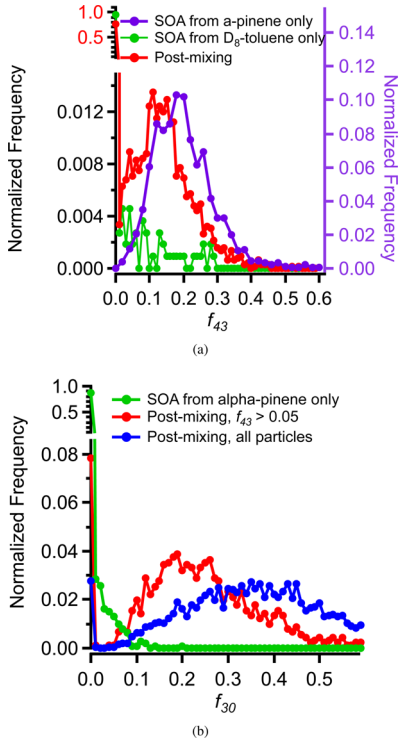

Figure 10. (a) Normalized histogram of distribution of f_{43} within single particles for the α-pinene SOA and toluene-d_8 SOA mixing experiment, and a pure α-pinene SOA dilution experiment. The fraction of the α-pinene marker fragment shifts to lower values with the incorporation of non-α-pinene SOA molecules entering the particles. (b) Normalized histogram of distribution of f_{30} for pure aP SOA particles from a control experiment, as well as single particles from the α-pinene SOA and toluene-d_8 SOA mixing experiment. Separate traces are shown for all single particles in the mixing experiment, as well as single particles with significant m/z 43 (orignially aP SOA).

in Figure 10a, so all particles with significant f_{43} are SOA particles originally from α-pinene oxidation. When those α-pinene-derived particles enter a chamber containing toluene-d_8-derived SOA, the peak in the histogram shifts from 0.2 to 0.12. This indicates that approximately 40% of the mass in the particles comes from toluene oxidation products, indicating a high degree of mixing throughout most of the volume of these particles. A similar histogram showing the distribution of f_{30} confirms that toluene-d_8 oxidation product fragments (for which m/z 30 is a unique tracer) condense onto SOA from α-pinene oxidation (Figure 10b). SOA from α-pinene oxidation in our control experiment shows practically no signal from m/z 30. However, there is significant m/z 30 in the α-pinene SOA (determined by filtering the single-particle mass spectra for f_{43} > 0.05) after the mixing event.

Because the mass size distributions for the two SOA populations have unique mass spectral fragments that distinct in size, we are able to use PToF data to confirm our conclusions (as in Asa-Awuku et al.[15]). Figure 11 shows a toluene fragment (m/z 46) condensing onto the originally α-pinene-derived SOA particles.

The presence of toluene-d_8 oxidation products within the SOA from α-pinene oxidation must be from absorption of those vapors into the particles. Coagulation is ruled out, as previously explained for above experiments, as an important mixing process for its long time scale. Adsorption is ruled out

dx.doi.org/10.1021/jp405789t | J. Phys. Chem. A 2013, 117, 13935−13945

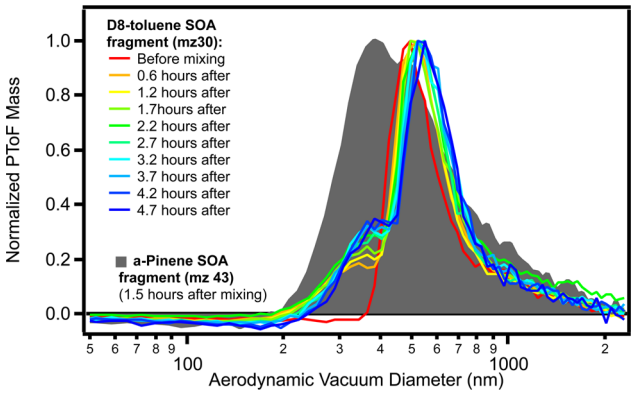

Figure 11. Time evolution of normalized mass distributions for m/z 30, a marker fragment for toluene-d_8 SOA. The α-pinene SOA marker fragment (m/z 43) is plotted in the background to show how toluene-d_8 SOA molecules are condensing onto the α-pinene SOA mode.

because there is no driving force for residual vapors to adsorb onto the SOA from α-pinene, as there is not a supersaturation of toluene-d_8 oxidation products in the chambers. Thus, the presence of oxidized toluene-d_8 molecules at the mass fraction of ~40%, very strongly indicates that there is absorption into the α-pinene SOA particles.

Interestingly, almost no mixing occurs in the other direction. As shown by the strong band of particles with high correlation to the toluene-d_8 SOA reference, few of these toluene particles receive α-pinene SOA molecules. The majority (over 70%) of particles with correlation >0.8 have no m/z 43 in them at all. It is possible that there were few, if any, α-pinene SOA vapors available for condensation into the toluene-d_8 SOA. Other studies have shown diluted α-pinene SOA to evaporate slowly, on multihour time scales, due either to (1) very low internal diffusivities for organic molecules trying to escape the condensed phase and reach the new equilibrium dictated by the dilution[10] or (2) some other long time scale process, such as the decomposition of oligomeric species.[40] We can say with confidence that some fraction (if not all) of an α-pinene SOA particle does not have extremely low internal diffusivity, characteristic of crystalline solids or glasses. We draw this conclusion because toluene-d_8 SOA molecules are able to enter the α-pinene-derived SOA particles rapidly (in minutes). It remains possible that some fraction of the α-pinene SOA particles do not absorb toluene oxidation product vapors, but our measurements do not allow us to answer this question nor diagnose a particle morphology.

CONCLUSIONS

Particle mixing dynamics are critically important to the evolution of organic aerosols in the atmosphere. The data presented here show that single-particle mass spectra from LSSP operation of the HR-ToF-AMS are extremely effective at elucidating the mixing dynamics of aerosol populations. Indeed, we present experiments where any mixing behavior happening would be invisible to the normal ensemble measurement techniques.

Distinct particle populations will mix when there is a thermodynamic driving force to do so. This happens at a rate no faster than a maximum determined by the volatility of constituents comprising the particles. The rate may be slower if there are substantial barriers to mass transfer, such as accommodating into crystal lattices or diffusing through a highly viscous condensed phase. It is important to distinguish between thermodynamic versus kinetic reasons for nonmixing. That is, particle populations that slowly mix (or do not mix at all) because they are immiscible must be distinguished from those that mix slowly because of other mass-transfer limitations. Thus, when experiments reveal relatively rapid mixing, there is little or no ambiguity about potential mass-transfer limitations. When mixing is slow, one can conclude that condensed phase mass-transfer limitations exist only when volatility limitations to mixing have been ruled out. We have shown examples of each situation.

By employing single-component particle populations containing isotopically labeled molecules of known volatility, we have been able to identify systems that mix according to expectation and others that show clear limitations to mass transfer. Populations composed of hydrogenated and deuterated squalane (30 carbon liquid oil) mix with each other slowly over the course of many hours, at a rate consistent with the (extremely low) saturation mass concentration of the squalane. This serves to illustrate just how low saturation vapor pressures must be for molecules to stay in particles under ambient conditions. Conversely, populations of particles containing much lower molecular weight hydrogenated and deuterated docosane (22 carbon paraffin wax) fail to show any signs of mixing for many hours at room temperature. This is true even though the saturation concentration of docosane vapors above solid docosane is much higher than that of squalane vapors over liquid squalane. When heated above the melting point of the docosane, however, the hydrogenated and deuterated docosane particle populations mix rapidly. Because docosane vapors also mix into liquid squalane particles at room temperature, this indicates clearly that mass-transfer limitations do exist for uptake of docosane vapors into crystalline docosane particles.

In the atmosphere, particle populations are complex mixtures, and in many cases they contain highly oxidized secondary organic constituents. It is these oxidized molecules that have most frequently been associated with highly viscous glassy states in particles;[10,17,41] SOA derived from α-pinene has been identified as slow to evaporate[10] and by implication glassy.

Here we have shown that particle populations composed of biogenic SOA derived from ozonolysis of α-pinene and anthropogenic SOA derived from OH oxidation of (deuterated) toluene are able to mix quickly. Specifically, vapors derived from deuterated toluene are able to mix into particles derived from α-pinene very quickly. Those same toluene-derived vapors show no sign of mixing into particles of pure squalane, suggesting that the lack of mixing in the presence of toluene-derived vapors indicates a thermodynamic inhibition (they are simply immiscible), rather than a mass-transfer limitation to uptake. There is thus no evidence that these α-pinene-derived SOA particles had any substantial mass-transfer limitations delaying vapor uptake.

The same mixing experiments that revealed rapid mixing of toluene-derived vapors into α-pinene-derived SOA particles did not show mass transfer going the other way. There was no uptake of α-pinene-derived vapors into particles derived from toluene oxidation. The reasons for this remain unknown. It may be that the vapor concentration of the diluted α-pinene ozonolysis products are simply too low (possibly because the α-pinene-derived particles are not volatile enough to produce them), or it may be because the toluene-derived particles raise barriers to the uptake of those vapors. Recent experimental[42] and modeling[43] work from our group suggest that the volatility

distribution of α-pinene-derived SOA may be lower than reported previously from SOA formation studies.[44] Whether the lack of penetration into the toluene-d_8-derived SOA by molecules from α-pinene oxidation is due to low volatility, diffusion limitations or mass-transfer barriers, or is simply an issue of miscibility, is a question being pursued in future work.

The experiments described here reveal that answers to questions such as "are SOA particles glassy?" or "does ambient organic aerosol reach equilibrium rapidly in the atmosphere?" are complex and the answers likely depend on the specific characteristics of the mixtures in question. We must take great care to avoid generalizations about either the presence or absence of equilibrium behavior and take great pains to understand these systems under conditions that come as close as possible to those found in the real atmosphere. The biogenic α-pinene SOA system is a de facto model for SOA in both experimental studies and chemical transport models, and the experiments described here reveal that these particles can rapidly uptake vapors from an external source. Though not a direct measurement of equilibrium, these data do show that diffusion in SOA from α-pinene ozonolysis should not impede equilibrium partitioning. Other recent studies[42,45] that do measure equilibrium time scales in SOA systems show that they are short. There is thus no compelling reason to rush to judgment that all organic aerosol systems are necessarily slow to equilibrate under ambient conditions, but there is certainly a compelling reason to continue to probe the question of when systems are likely to move slowly toward equilibrium and how the equilibrium time scale significantly influences important aerosol properties, like mixing.

■ ASSOCIATED CONTENT

Supporting Information

Justification for assuming that coagulation is not a significant mixing process is presented, as well as additional condensational mixing model results, a docosane/D_{62}-squalane mixing experiment, and a comparison of average single-particle mass spectra with the V-mode mass spectrum from normal HR-ToF-AMS operation. This material is available free of charge via the Internet at http://pubs.acs.org.

■ AUTHOR INFORMATION

Corresponding Author

*N. M. Donahue: e-mail, nmd@cmu.edu.

Notes

The authors declare no competing financial interest.

Biographies

Ellis Robinson is a graduate student in the Center for Atmospheric Particle Studies at Carnegie Mellon University. His primary research focus is on the mixing and phase state of organic aerosol classes, with emphasis on experimental smog chamber studies using single-particle mass spectrometry. He holds a B.S. in Chemical and Biomolecular Engineering from The Ohio State University and was a 2013 AAAS Mass Media Fellow at Aspen Public Radio.

Rawad Saleh is a postdoctoral researcher in the Center for Atmospheric Particle Studies at Carnegie Mellon University. He holds a B.Sc. and M.Sc. in Mechanical Engineering from the Middle East Technical University and the American University of Beirut, and a Ph.D. in Environmental Engineering from Duke University. His research focuses on organic aerosol partitioning kinetics and thermodynamics, as well as optical properties of light-absorbing particles (black carbon and brown carbon).

Neil Donahue directs the Steinbrenner Institute for Environmental Education and Research at Carnegie Mellon University. He is a cofounder and first director of the Center for Atmospheric Particle Studies and Professor in the departments of Chemistry, Chemical Engineering, and Engineering and Public Policy. He received an A.B. in Physics from Brown University and a Ph.D. in Meteorology from MIT. In recent years his research interests have focused on the coupling between gas-phase oxidation chemistry of organic compounds and their interactions with atmospheric particles. This includes equilibrium phase partitioning as well as the dynamics of condensation and evaporation for both bulk aerosol and freshly nucleated particles.

■ ACKNOWLEDGMENTS

This research was supported by grant CHE1012293 from the National Science Foundation. The High-Resolution Aerosol Mass Spectrometer was purchased with Major Research Instrumentation funds from NSF CBET0922643.

■ REFERENCES

(1) Lozano, R.; Naghavi, M.; Foreman, K.; Lim, S.; Shibuya, K.; Aboyans, V.; Abraham, J.; Adair, T.; Aggarwal, R.; Ahn, S. Y. Global and regional mortality from 235 causes of death for 20 age groups in 1990 and 2010: a systematic analysis for the Global Burden of Disease Study 2010. *Lancet* **2013**, *380*, 2095−2128.

(2) Pope, C. A., III; Ezzati, M.; Dockery, D. W. Fine-particulate air pollution and life expectancy in the United States. *N. Engl. J. Med.* **2009**, *360*, 376−386.

(3) Solomon, S.; Qin, D.; Manning, M.; Alley, R. B.; Berntsen, T.; Bindoff, N. L.; Chen, Z.; Chidthaisong, A.; Gregory, J. M.; Hegerl, G. C. *Climate change 2007: The physical science basis, contribution of working group 1 to the fourth assessment report of the Intergovernmental Panel on Climate Change*; Cambridge University Press: Cambridge, U.K., 2007; http://www.ipcc.ch/publications_and_data/ar4/wg1/en/contents.html.

(4) Showstack, R. The Perfect Haze: Scientists Link 1999 U.S. Pollution Episode to Midwest Aerosol Plumes and Kennedy Plane Crash. *EOS, Trans. Am. Geophys. Union* **2000**, *81*, 13−14.

(5) Jimenez, J. L.; et al. Evolution of Organic Aerosols in the Atmosphere. *Science* **2009**, *326*, 1525−1529.

(6) Kanakidou, M.; Seinfeld, J. H.; Pandis, S. N.; Barnes, I.; Dentener, F. J.; Facchini, M. C.; Van Dingenen, R.; Ervens, B.; Nenes, A.; Nielsen, C. J. Organic aerosol and global climate modelling: a review. *Atmos. Chem. Phys.* **2005**, *5*, 1053−1123.

(7) Goldstein, A. H.; Galbally, I. E. Known and unexplored organic constituents in the earth's atmosphere. *Environ. Sci. Technol.* **2007**, *41*, 1514−1521.

(8) Donahue, N. M.; Epstein, S. A.; Pandis, S. N.; Robinson, A. L. A two-dimensional volatility basis set: 1. organic-aerosol mixing thermodynamics. *Atmos. Chem. Phys.* **2011**, *11*, 3303−3318.

(9) Renbaum-Wolff, L.; Grayson, J. W.; Bateman, A. P.; Kuwata, M.; Sellier, M.; Murray, B. J.; Shilling, J. E.; Martin, S. T.; Bertram, A. K. Viscosity of alpha-pinene secondary organic material and implications for particle growth and reactivity. *Proc. Natl. Acad. Sci. U. S. A.* **2013**, *110*, 8014−8019.

(10) Vaden, T.; Imre, D.; Beránek, J.; Shrivastava, M.; Zelenyuk, A. Evaporation kinetics and phase of laboratory and ambient secondary organic aerosol. *Proc. Natl. Acad. Sci. U. S. A.* **2011**, *108*, 2190−2195.

(11) Perraud, V.; Bruns, E.; Ezell, M.; Johnson, S.; Yu, Y.; Alexander, M.; Zelenyuk, A.; Imre, D.; Chang, W.; Dabdub, D. Nonequilibrium atmospheric secondary organic aerosol formation and growth. *Proc. Natl. Acad. Sci. U. S. A.* **2012**, *109*, 2836−2841.

(12) Song, C.; Zaveri, R. A.; Alexander, M. L.; Thornton, J. A.; Madronich, S.; Ortega, J. V.; Zelenyuk, A.; Yu, X.-Y.; Laskin, A.; Maughan, D. A. Effect of hydrophobic primary organic aerosols on secondary organic aerosol formation from ozonolysis of alpha-pinene. *Geophys. Res. Lett.* **2007**, *34*, L20803.

(13) Hildebrandt, L.; Henry, K. M.; Kroll, J. H.; Worsnop, D. R.; Pandis, S. N.; Donahue, N. M. Evaluating the Mixing of Organic Aerosol Components Using High-Resolution Aerosol Mass Spectrometry. *Environ. Sci. Technol.* **2011**, *45*, 6329−6335.
(14) Vaden, T.; Song, C.; Zaveri, R. A.; Imre, D.; Zelenyuk, A. Morphology of mixed primary and secondary organic particles and the adsorption of spectator organic gases during aerosol formation. *Proc. Natl. Acad. Sci. U. S. A.* **2010**, *107*, 6658−6663.
(15) Asa-Awuku, A.; Miracolo, M. A.; Kroll, J. H.; Robinson, A. L.; Donahue, N. M. Mixing and phase partitioning of primary and secondary organic aerosols. *Geophys. Res. Lett.* **2009**, *36*.
(16) Cappa, C. D.; Wilson, K. R. Evolution of organic aerosol mass spectra upon heating: implications for OA phase and partitioning behavior. *Atmos. Chem. Phys.* **2011**, *11*, 1895−1911.
(17) Koop, T.; Bookhold, J.; Shiraiwa, M.; Pöschl, U. Glass transition and phase state of organic compounds: dependency on molecular properties and implications for secondary organic aerosols in the atmosphere. *Phys. Chem. Chem. Phys.* **2011**, *13*, 19238.
(18) Marcolli, C.; Luo, B.; Peter, T.; Wienhold, F. Internal mixing of the organic aerosol by gas phase diffusion of semivolatile organic compounds. *Atmos. Chem. Phys.* **2004**, *4*, 2593−2599.
(19) Smith, M. L.; Bertram, A. K.; Martin, S. T. Deliquescence, efflorescence, and phase miscibility of mixed particles of ammonium sulfate and isoprene-derived secondary organic material. *Atmos. Chem. Phys.* **2012**, *12*, 9613−9628.
(20) Bertram, A. K.; Martin, S. T.; Hanna, S. J.; Smith, M. L.; Bodsworth, A.; Chen, Q.; Kuwata, M.; Liu, A.; You, Y.; Zorn, S. R. Predicting the relative humidities of liquid-liquid phase separation, efflorescence, and deliquescence of mixed particles of ammonium sulfate, organic material, and water using the organic-to-sulfate mass ratio of the particle and the oxygen-to-carbon elemental ratio of the organic component. *Atmos. Chem. Phys.* **2011**, *11*, 10995−11006.
(21) Marcolli, C.; Krieger, U. K. Phase Changes during Hygroscopic Cycles of Mixed Organic/Inorganic Model Systems of Tropospheric Aerosols. *J. Phys. Chem. A* **2006**, *110*, 1881−1893.
(22) Donahue, N. M.; Robinson, A. L.; Stanier, C. O.; Pandis, S. N. Coupled Partitioning, Dilution, and Chemical Aging of Semivolatile Organics. *Environ. Sci. Technol.* **2006**, *40*, 2635−2643.
(23) Robinson, A. L.; Donahue, N. M.; Shrivastava, M. K.; Weitkamp, E. A.; Sage, A. M.; Grieshop, A. P.; Lane, T. E.; Pierce, J. R.; Pandis, S. N. Rethinking Organic Aerosols: Semivolatile Emissions and Photochemical Aging. *Science* **2007**, *315*, 1259−1262.
(24) Odum, J. R.; Hoffmann, T.; Bowman, F.; Collins, D.; Flagan, R. C.; Seinfeld, J. H. Gas/particle partitioning and secondary organic aerosol yields. *Environ. Sci. Technol.* **1996**, *30*, 2580−2585.
(25) Presto, A. A.; Donahue, N. M. Investigation of alpha-Pinene + Ozone Secondary Organic Aerosol Formation at Low Total Aerosol Mass. *Environ. Sci. Technol.* **2006**, *40*, 3536−3543.
(26) Grieshop, A. P.; Miracolo, M. A.; Donahue, N. M.; Robinson, A. L. Constraining the Volatility Distribution and Gas-Particle Partitioning of Combustion Aerosols Using Isothermal Dilution and Thermodenuder Measurements. *Environ. Sci. Technol.* **2009**, *43*, 4750−4756.
(27) Kroll, J. H.; Smith, J. D.; Che, D. L.; Kessler, S. H.; Worsnop, D. R.; Wilson, K. R. Measurement of fragmentation and functionalization pathways in the heterogeneous oxidation of oxidized organic aerosol. *Phys. Chem. Chem. Phys.* **2009**, *11*, 8005.
(28) Weitkamp, E. A.; Sage, A. M.; Pierce, J. R.; Donahue, N. M.; Robinson, A. L. Organic Aerosol Formation from Photochemical Oxidation of Diesel Exhaust in a Smog Chamber. *Environ. Sci. Technol.* **2007**, *41*, 6969−6975.
(29) Cross, E.; Onasch, T.; Canagaratna, M.; Jayne, J.; Kimmel, J.; Yu, X.; Alexander, M.; Worsnop, D.; Davidovits, P. Single particle characterization using a light scattering module coupled to a time-of-flight aerosol mass spectrometer. *Atmos. Chem. Phys.* **2009**, *9*, 7769−7793.
(30) Sparrow 1.04A, written by D. Sueper, Aerodyne Research Inc. and University of Colorado at Boulder; available at http://cires.colorado.edu/jimenez-group/ ToFAMSResources/ToFSoftware/index.htmlAnalysis4.
(31) Liu, S.; Russell, L. M.; Sueper, D. T.; Onasch, T. B. Organic particle types by single-particle measurements using a time-of-flight aerosol mass spectrometer coupled with a light scattering module. *Atmos. Meas. Tech.* **2013**, *6*, 187−197.
(32) Pankow, J.; Asher, W. SIMPOL. 1: a simple group contribution method for predicting vapor pressures and enthalpies of vaporization of multifunctional organic compounds. *Atmos. Chem. Phys.* **2008**, *8*, 2773−2796.
(33) Somorjai, G. A.; Lester, J. E. Evaporation mechanism of solids. *Prog. Solid State Chem.* **1967**, *4*, 1−52.
(34) Pandis, S. N.; Harley, R. A.; Cass, G. R.; Seinfeld, J. H. Secondary organic aerosol formation and transport. *Atmos. Environ.* **1992**, *26*, 2269−2282.
(35) Baltaretu, C. O.; Lichtman, E. I.; Hadler, A. B.; Elrod, M. J. Primary Atmospheric Oxidation Mechanism for Toluene. *J. Phys. Chem. A* **2009**, *113*, 221−230.
(36) Robinson, A. L.; Grieshop, A. P.; Donahue, N. M.; Hunt, S. W. Updating the Conceptual Model for Fine Particle Mass Emissions from Combustion Systems. *J. Air Waste Manage. Assoc.* **2010**, *60*, 1204−1222.
(37) Donahue, N. M.; Chuang, W.; Epstein, S. A.; Kroll, J. H.; Worsnop, D. R.; Robinson, A. L.; Adams, P. J.; Pandis, S. N. Why do organic aerosols exist? Understanding aerosol lifetimes using the two-dimensional volatility basis set. *Environ. Chem.* **2013**, *10*, 151.
(38) Hennigan, C. J.; Sullivan, A. P.; Collett, J. L., Jr.; Robinson, A. L. Levoglucosan stability in biomass burning particles exposed to hydroxyl radicals. *Geophys. Res. Lett.* **2010**, *37*, L09806.
(39) Presto, A. A.; Miracolo, M. A.; Donahue, N. M.; Robinson, A. L. Secondary Organic Aerosol Formation from High-NO xPhoto-Oxidation of Low Volatility Precursors: n-Alkanes. *Environ. Sci. Technol.* **2010**, *44*, 2029−2034.
(40) Grieshop, A. P.; Donahue, N. M.; Robinson, A. L. Is the gas-particle partitioning in alpha-pinene secondary organic aerosol reversible. *Geo. Res. Let.* **2007**, *34*.
(41) Zobrist, B.; Marcolli, C.; Pedernera, D.; T, K. Do atmospheric aerosols form glasses? *Atmos. Chem. Phys.* **2008**, *8*, 5221−5244.
(42) Saleh, R.; Donahue, N. M.; Robinson, A. L. Time Scales for Gas-Particle Partitioning Equilibration of Secondary Organic Aerosol Formed from Alpha-Pinene Ozonolysis. *Environ. Sci. Technol.* **2013**, 130517130052009.
(43) Trump, E.; Donahue, N. M. Oligomer formation within secondary organic aerosol: equilibrium and dynamic considerations. *Atmos. Chem. Phys.* 2013, *13*, 24605−24634.
(44) Pathak, R. K.; PResto, A. A.; Lane, T. E.; Stanier, C. O.; Donahue, N. M.; Pandis, S. N. Ozonolysis of α-pinene: parameterization of secondary organic aerosol mass fraction. *Atmos. Chem. Phys.* **2007**, *7*, 3811−3821.
(45) Yatavelli, R. L. N.; Stark, H.; Thompson, S. L.; Kimmel, J. R.; Cubison, M. J.; Day, D. A.; Campuzano-Jost, P.; Palm, B. B.; Thornton, J. A.; Jayne, J.; Worsnop, D. R.; Jimenez, J. L. Semi-continuous measurements of gas/particle partitioning of organic acids in a ponderosa pine forest using a MOVI-HRToF-CIMS. *Atmos. Chem. Phys. Discuss.* **2013**, *13*, 17327−17374.